

Oligo(*p*-phenyleneethynylene)-functionalized Perylenebis-imidetriad: Synthesis, Photophysical Properties, and Self-assembly

Weiqi Tong,^a Wei Wei,^b Haibo Chen,^c and Hongyu Wang^{*a}

^a Department of Chemistry, Shanghai University, Shanghai 200444, China

^b Institute of Advanced Materials, Nanjing University of Posts and Telecommunications, Nanjing, Jiangsu 210003, China

^c Downhole Operation Team, Second Oil Extraction Factory, Zhongyuan Petro Oil Exploration Bureau, Puyang, Henan 457001, China

The rod-like oligo(*p*-phenylene ethynylene)-functionalized perylene bisimide triad was synthesized and characterized. Aggregation behavior in solvents of different polarity was investigated by absorption and fluorescent spectroscopy. The results showed that stronger aggregations took place in low-polarity solvent. The experiments also indicated that the energy and electron transfer might take place between the two chromophores during the photoinduced excitation. Highly ordered two-dimensional assemblies could be observed at solid/liquid interfaces.

Keywords perylenebisimide, donor-acceptor, energy transfer, electron transfer, self-assembly

Introduction

Inspired by natural photosynthetic reaction centers, which contain chlorophyll dyes as electron donor and quinones as electron acceptors, perylenebisimides (PBIs) have become one of the most popular building blocks to construct donor-acceptor (D-A) architecture for photophysical studies.^[1,2] However, perylenebisimide derivatives appear to be more powerful electron acceptor than quinones, since they can be easily connected to various scaffolds via the imide nitrogens, and their optical and redox properties can be easily tuned over a wide range by molecular structure design, especially by appropriate choice of the substituents in the “bay” area.^[3,4] By using a variety of binding motifs (*e.g.* covalent linkages, hydrogen bonds, metal ion coordination and π - π stacking), a large number of functional systems and assemblies based on PBIs have been developed.^[5-7] Particularly, Wasielewski group and Würthner group have recognized these advantageous features of mono- and bisimide chromophores and exploited them for a broad variety of photophysical studies on dyad and triad molecules.^[8,9]

In our previous work,^[10] we reported the alternative copolymers based on oligo(*p*-phenyleneethynylene) (OPE) and PBIs units, which exhibited efficient photo induced energy and electron transfer from photo excited OPE unit to PBI. The ideal features of OPE for con-

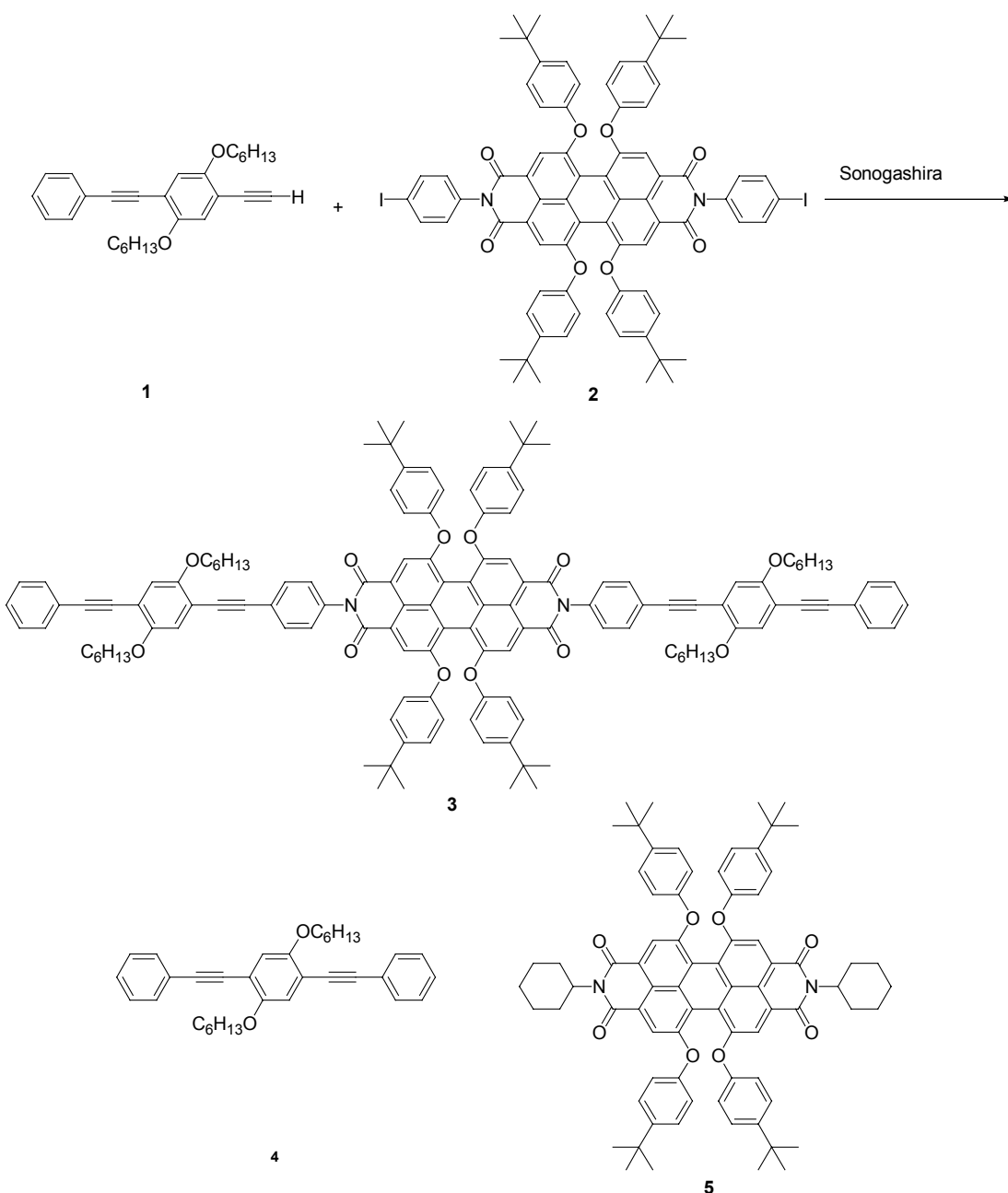
structing D-A architecture with PBIs exhibit the following attributes: (1) The absorption of OPE is a complementation to PBIs, and the absorption of the copolymers almost cover the whole visible region. (2) Cylindrical symmetry of the acetylene unit maintains the π -electron conjugation at any degree of rotation. And the rigid rod-like character of phenylene-ethynlenes has ability to communicate charge/excitation energy over long distances.^[11] (3) The solubility of PBIs can be efficiently increased by introducing OPE unit.

The synthesis and investigation of structurally defined conjugated oligomers as models for the corresponding polymers will lead to more valuable structure property relationships. In this respect, we report the synthesis, characterization, and photophysical studies of a novel D-A-D triad **3** carrying OPE as the electron donor and perylenebisimide as the electron acceptor. The optical and electrochemical properties of the triad were carefully investigated using UV-vis absorption and fluorescence spectroscopy. In order to evaluate the influence on photophysical properties of introduction of OPE unit to perylenebisimide core, two model compounds 1,4-bis(phenylethynyl)-2,5-bis(hexyloxy)benzene **4** and *N,N'*-dicyclohexyl-1,6,7,12-tetrakis(4-*tert*-butylphenoxy)-3,4:9,10-perylenedicarboximide **5** were synthesized. Furthermore, the scanning tunneling microscopy (STM) was carried out to understand the intermolecular interactions, which are essential for device fabrication.

* E-mail: wanghy@shu.edu.cn; Tel.: 0086-021-66135108

Received August 23, 2012; accepted November 1, 2012; published online December 11, 2012.

Supporting information for this article is available on the WWW under <http://dx.doi.org/10.1002/cjoc.201200858> or from the author.

Scheme 1 Synthetic route of the triad **3** and chemical structure of models **4** and **5**

Experimental

Unless otherwise stated, reagents were commercially obtained and used without further purification. The solvents for cross-coupling reaction were purified according to the standard methods. The synthetic procedures of **1**, **2**, **4** and **5** have been published previously.^[10,12-14]

The NMR spectra were recorded on a Varian Mercury Plus 400 spectrometer with tetramethylsilane as the internal standard. Matrix-assisted laser desorption ionization-time-of-flight mass (MALDI-TOF) experiments were carried out using a Shimadzu AXIMA-CFR™ plus time-of-flight mass spectrometer (Kratos Analytical, Manchester, U. K.). Thermogravimetric analysis (TGA) was performed on a Shimadzu thermogravimetry

and differential thermal analysis DTG-60H at a heating rate of $10\text{ }^{\circ}\text{C}\cdot\text{min}^{-1}$ under N_2 . Differential scanning calorimetry (DSC) measurements were performed under a nitrogen atmosphere at heating rates of $10\text{ }^{\circ}\text{C}\cdot\text{min}^{-1}$, using NETZSCH DSC 200PC apparatus. UV-vis spectra were recorded on a Shimadzu 3150 PC spectrophotometer. Fluorescence measurement was carried out on a Shimadzu RF-5301 PC spectrofluorophotometer with a xenon lamp as a light source. Cyclic voltammetry (CV) was performed at a scanning rate of $100\text{ mV}\cdot\text{s}^{-1}$ on an AUTOLAB PGSTAT30 potentiostat/galvanostat system (Ecochemie, Netherlands), which was equipped with a three-electrode cell. The glass carbon electrode was used as the working electrode and Pt wire was used

as the counter electrode. An Ag/Ag⁺ was used as a reference electrode. 0.1 mol/L tetrabutyl ammonium hexafluorophosphate (*n*-Bu₄NPF₆) was used as a supporting electrolyte. The dichloromethane solution of oligomer was cast onto the glass carbon disk as a working electrode and determined in acetonitrile. Scanning tunneling microscope (STM) measurements were performed with a Nanoscope IIIa (Veeco Metrology, USA) with mechanically formed Pt/Ir (80/20) tips. A droplet (2 μL) of *n*-octylbenzenesolution containing **3** at a concentration of approximately 10⁻⁶ mol/L was dropped on freshly cleaved highly oriented pyrolytic graphite (HOPG) (grade ZYB, eeco Metrology, USA) surface and investigated by STM immediately. All images were recorded in constant current mode.

Synthesis of the triad **3**

Monomer **1** (44.3 mg, 0.11 mmol), **2** (69.4 mg, 0.05 mmol), tetrakis(triphenylphosphine) palladium (4 mg), and CuI (2 mg) were added to a mixture of THF (5 mL) and diisopropylamine (5 mL). The mixture was vigorously stirred at 50 °C for 48 h under nitrogen. After cooling to room temperature and removal of the solvent under reduced pressure, the residue was purified by column chromatography using a mixture of dichloromethane and hexane (*V/V*=6 : 4) as eluent to afford **3** (78.9 mg, 72%) as dark red powder. ¹H NMR (400 MHz, CDCl₃) δ: 8.26 (s, 4H), 7.64 (d, *J*=8 Hz, 4H), 7.54–7.51 (m, 4H), 7.34–7.32 (m, 6H), 7.25–7.23 (m, 12H), 7.02 (d, *J*=4.4 Hz, 4H), 6.85 (d, *J*=8.4 Hz, 8H), 4.0 (t, *J*=6.4, 8H), 1.82–1.84 (m, 8H), 1.34–1.38 (m, 24H), 1.24 (s, 36H), 0.89–0.90 (m, 12H); ¹³C NMR (400 MHz, CDCl₃) δ: 163.66, 156.36, 153.95, 153.83, 152.97, 147.70, 139.51, 135.12, 133.36, 132.60, 131.80, 128.90, 128.52, 126.94, 124.95, 124.69, 124.29, 123.67, 122.65, 121.03, 120.41, 119.96, 119.58, 117.18, 117.10, 114.41, 113.86, 95.15, 94.33, 87.18, 86.17, 69.86, 69.82, 34.60, 34.07, 32.17, 31.85, 31.66, 30.55, 30.43, 29.94, 25.98, 22.88, 14.30. MASS (MALDI-TOF): 1937.8 (calcd for C₁₃₂H₁₃₀N₂O₁₂: 1936.4).

Results and Discussion

Characterization

The triad **3** was synthesized by Hagihara-Sonogashira cross-coupling reaction in a tetrahydrofuran/diisopropylamine mixture. The results from ¹H NMR, ¹³C NMR and MALDI-TOF mass analysis confirmed that the synthesized compounds have the predicted chemical structures. The NMR spectra and MALDI-TOF mass spectra of the triad **3** were shown in the supporting information (Figures S1–S3). The ¹H NMR characteristic peaks of the oligomer at δ 8.26 are due to the resonance of protons on perylene ring, and the triplet peaks at δ 4.0 are due to the resonance of protons on methylene adjacent to the oxygen atoms of alkoxy chains. But the signals of protons of acetylene group at δ 3.34 in monomer **1** could no longer be detected in **3**.

The triad **3** has molecular weight of 1937.8 determined by MALDI-TOF mass, which is consistent with the real molecular weight. According to thermal gravimetric analysis (TGA), the triad **3** has fair thermal stability. The onset of thermal degradation under a nitrogen atmosphere was recorded at 353 °C (5% weight loss). No glass transition temperature, *T_g*, was obtained for the oligomer by DSC measurement while heating to 250 °C.

Aggregation behavior in solutions

The aggregation behavior of triad **3** was studied in detail by UV-vis absorption and fluorescence spectroscopy in polar solvent dichloromethane and nonpolar solvent hexane (Figures 1–4). The absorption bands of the PBI chromophore give three characteristic peaks at longer wavelength from 450 to 600 nm,^[15] while the absorption bands of the OPE chromophore appear at 370 nm.^[12] In hexane solution, upon increasing the concentration (Figure 1), the absorption maxima of PBI chromophore was red-shifted by about 26 nm. And aggregation-induced broadening was also observed, while the fine structure remained almost the same. The absorption spectra of the aggregated triad **3** agreed remarkably well with the four phenoxy substituents in the bay positions of perylene derivatives reported by Würthner.^[16] However, the absorption spectra of **3** in DCM almost unchanged upon increasing the concentration to 5×10⁻⁵ mol/L (Figure 2).

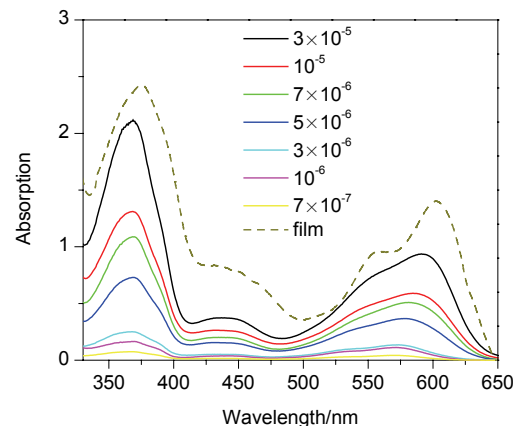


Figure 1 Concentration-dependent UV-vis absorption spectra of **3** in hexane (concentration range 7×10⁻⁷–3×10⁻⁵ mol/L). Dotted line represents the spectrum of absorption in thin films.

Fluorescence spectroscopy of DCM solutions showed a significant red shift (about 13 nm) of the emission maxima upon aggregation, with almost unaltered fine structure (Figure 3). An almost linear dependence of the fluorescence intensity on the concentration was observed until the concentration increased to 10⁻⁵ mol/L. The deviation from the linearity at higher concentrations could be described fully by the application of Beer's law to the excitation light in the sample (Figure 3, inset). This indicated that the aggregation has

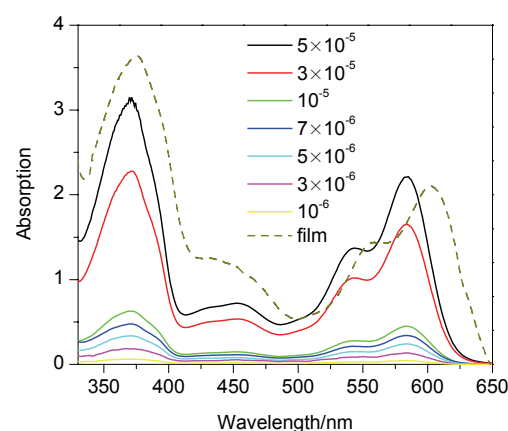


Figure 2 Concentration-dependent UV-vis absorption spectra of **3** in dichloromethane (concentration range 10^{-6} – 5×10^{-5} mol/L). Dotted line represents the spectrum of absorption in thin films.

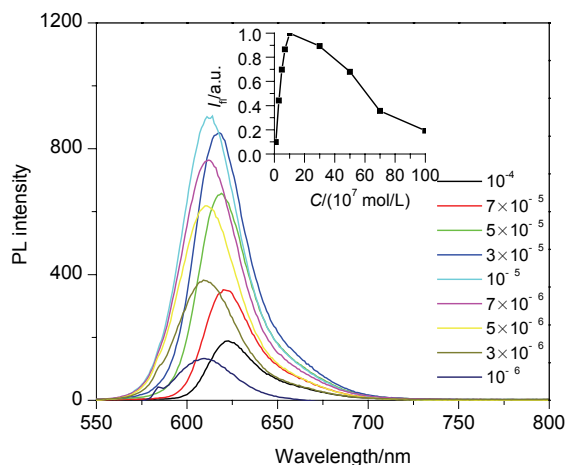


Figure 3 Concentration-dependent fluorescence spectra of **3** in DCM (concentration range 10^{-6} – 10^{-4} mol/L). Inset: dependence of the fluorescence intensity I_f on the concentration.

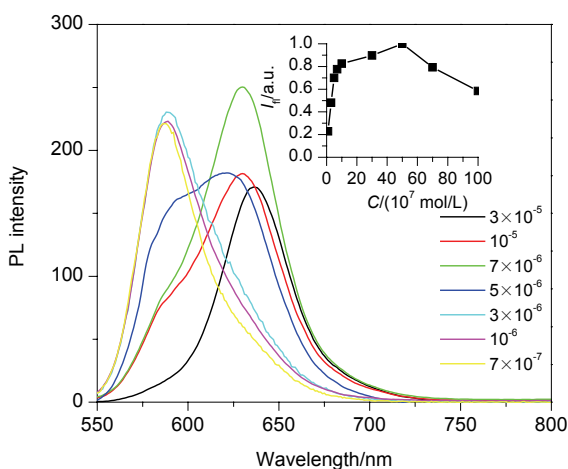


Figure 4 Concentration-dependent fluorescence spectra of **3** in hexane (concentration range 7×10^{-7} – 3×10^{-5} mol/L). Inset: dependence of the fluorescence intensity I_f on the concentration.

a negligible influence on the fluorescence quantum yield. This result is well agreed with many extended π systems, including other PBI derivatives.^[16] In the low-polar hexane (Figure 4), when the concentration increased to 5×10^{-6} mol/L, a new aggregation emission peak at 621 nm was observed. Increasing concentration gradually to 3×10^{-5} mol/L, the aggregation emission peak red-shifted to 637 nm. While the emission peak at 588 nm gradually decreased and finally disappeared. Also, the spectrum recorded from thin films closely resembled those obtained from concentrated solutions. At the concentration higher than 3×10^{-6} mol/L, the dependence of the fluorescence intensity on the concentration deviated from the linearity. All those results showed strong aggregation of the triad **3** takes place in low-polarity environments.

Optical properties

In order to avoid intermolecular aggregation, UV-vis and fluorescence spectra were recorded in high-polarity dichloromethane at a concentration where no aggregation takes place ($c=1 \times 10^{-6}$ mol/L). The optical properties of triad are very close to that of the alternative copolymers reported previously.^[10] The absorption bands of the PBI chromophore give the characteristic π - π^* transitions at 453 nm (S0–S2 electronic transition), 542 and 584 nm (S0–S1 electronic transition),^[15] while the absorption bands of the OPE chromophore appear at 370 nm. The spectrum of the oligomer **3** is almost identical and close to a linear superposition of the spectra of **4** and **5**, except for a 12 nm red shift (Figure 5). This result demonstrates that there is no ground state electronic interaction between the two chromophores,^[17] which is mainly due to the nodes in the HOMO and LUMO at imide nitrogen.^[18] The emission spectra of the oligomer **3** were recorded upon selective excitation of the two chromophores (Figure 6). When excited at 370 nm, where the OPE chromophore absorbs strongly, the oligomer displays almost totally quenched OPE fluorescence and a weak emission from the low energy PBI

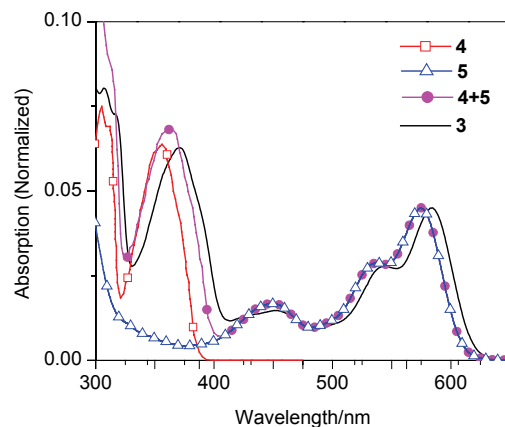


Figure 5 Absorption spectra of the triad **3**, models **4** and **5** in DCM (1×10^{-6} mol/L). The circles represent the spectrum of a 1 : 1 molar mixture of **4** and **5**.

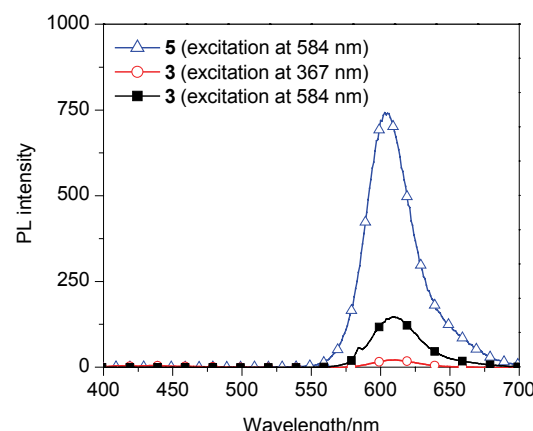


Figure 6 Fluorescence emission spectra of the triad **3**, and **5** in DCM (1×10^{-6} mol/L) upon excitation of the OPE chromophore at 370 nm and excitation of the PBI chromophore at 584 nm, respectively.

unit at 610 nm is observed. This indicates that there exist the energy and/or electron transfer between two chromophores. When excited at 584 nm, the PBI emission is also strongly quenched in comparison with the fluorescence spectrum of model **5**. Because the singlet excited state of the PBI unit lies below that of the OPE unit according to UV-vis absorption spectra, excitation of the PBI unit, only electron transfer occurs from the PBI unit to charge-separated state, resulting in quenching the PBI fluorescence.

Electrochemical properties

We carried out cyclic voltammogram to investigate the redox properties of the triad **3** (Figure 7). As we know, perylenebisimides are fairly electron-deficient dyes, which are easy to reduce and rather difficult to oxidize.^[18] With phenoxy electondonor substituents, the triad **3** exhibits reversible reduction and irreversible oxidation waves. The anodic scan showed that the onset of oxidation occurred at 0.84 eV. When scanning cathodically, **3** exhibited the onset potentials of reduction

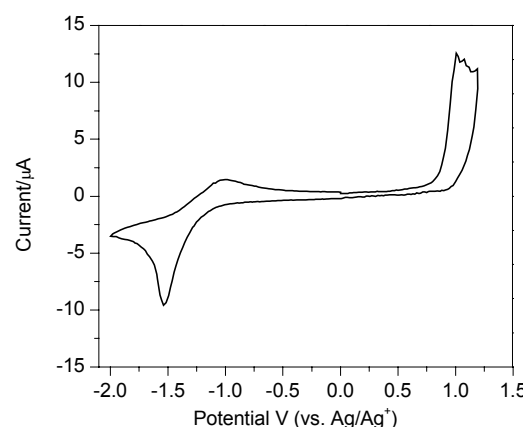


Figure 7 Cyclic voltammograms of the triad **3** recorded from a thin film deposited on an electrode in an electrolyte solution of Bu_4NPF_6 (0.1 mol/L) in CH_3CN at a scan rate of 100 mV/s.

at -1.14 eV. This oxidation and reduction potential is very close to the PBI monomer **5** ($E_{\text{ox}} = 0.78$ V and $E_{\text{red}} = -1.06$ V),^[10] which means the oxidation and reduction mainly take place in the PBI unit.

Self-assembly at the solid-liquid interface

In recent years, the self-assembly of complex multi-component molecules with tailored functionalities into highly ordered nanostructures attracts more attentions in the context of nanomaterials and nanotechnology.^[19] In particular, nanopatterning has become one of the major topics in these fields.^[20] The STM is a powerful tool to investigate two-dimensional organization of functionalized organic molecules at a solid-liquid interface, which provides access to molecular and supramolecular structure and dynamics on the single-molecule level.^[21] For example, DeFeyter and De Schryver have reported two-dimensional self-assembly of D-A triads based on perylenebisimides and oligo(*p*-phenylenevinylene)s (OPV₄-PDI-OPV₄)^[22] at solid-liquid interface. The two-dimensional self-assembly of **3** was presented. Figure 8 displays STM images of highly ordered monolayers of **3** at the solid-liquid interface on highly oriented pyrolytic

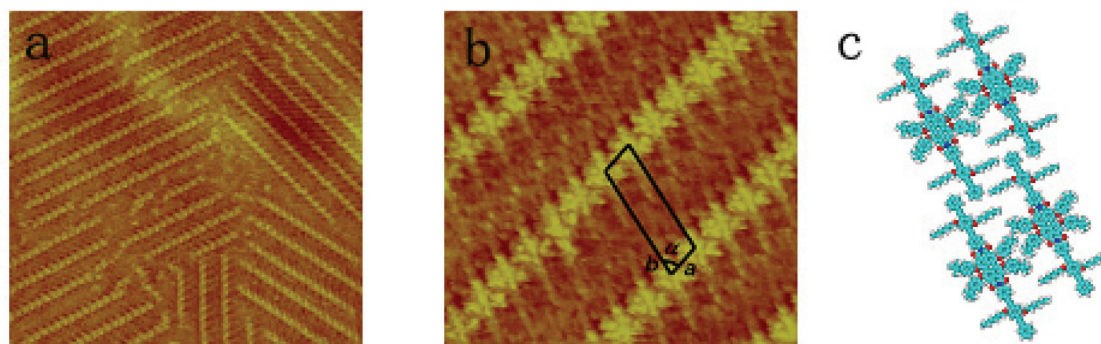


Figure 8 (a) Large-scale STM image ($76.5 \text{ nm} \times 76.5 \text{ nm}$) of **3**. The imaging conditions are $I=188.0$ pA and $V=-906.2$ mV. (b) A high-resolution STM image ($15.2 \text{ nm} \times 15.2 \text{ nm}$) of **3**. The imaging conditions are $I=156.6$ pA and $V=-941.3$ mV. (c) Structural model for **3**.

graphite (HOPG) under ambient conditions. Figure 8a shows the large uniform and well-ordered assembly. It is noticed that herringbone-shaped patterns are full of the whole viewed area. The details of the adlayer can be seen in a high-resolution STM image in Figure 8b. The adjacent molecules in the same rows are parallel to each other with a uniform bent direction. It is clear that the bright rods consist of three parts: the central part is attributed to the location of the PBI core part and the outermost parts correspond to the OPE moieties. A proposed model for the molecular arrangement could be shown in Figure 7c according to the STM image. The unit cell of the two dimensional (2D) assembly is superimposed on the molecular model with parameters $a = 2.0 \pm 0.1$ nm, $b = 5.1 \pm 0.2$ nm, $\alpha = 70^\circ \pm 2^\circ$.

Conclusions

In conclusion, we have synthesized a new OPE-PBI-OPE triad using the Sonogashira cross-coupling reaction. The aggregation behavior has been investigated by UV-vis absorption and fluorescent spectroscopy in hexane and dichloromethane. The stronger aggregation takes place in low-polarity hexane, when concentration reaches 3×10^{-6} mol/L. Excitation of the OPE unit in the triad results in photoinduced energy and electron transfers. Excitation of the PBI unit in the triad can only result in photoinduced electron transfer. Highly ordered two-dimensional assemblies can be obtained at solid/liquid interfaces.

References

- [1] Liu, H. B.; Li, Y. L.; Xiao, S. Q.; Gan, H. Y.; Jiu, T. G.; Li, H. M.; Jiang, L.; Zhu, D. B.; Yu, D. P.; Xiang, B.; Chen, Y. F. *J. Am. Chem. Soc.* **2003**, *125*, 10794.
- [2] Liu, H. B.; Xu, J. L.; Li, Y. J.; Li, Y. L. *Accounts Chem. Res.* **2010**, *43*, 1496.
- [3] Wang, C. Y.; Tang, W.; Zhong, H. B.; Zhang, X. C.; Shen, Y. J. *Chin. J. Chem.* **2009**, *27*, 2020.
- [4] Xiao, S. Q.; El-Khouly, M. E.; Li, Y. L.; Gan, Z. H.; Liu, H. B.; Jiang, L.; Araki, Y.; Ito, Q.; Zhu, D. B. *J. Phys. Chem. B* **2005**, *109*, 3658.
- [5] Qiu, W. F.; Chen, S. Y.; Sun, X. B.; Liu, Y. Q.; Zhu, D. B. *Org. Lett.* **2006**, *8*, 867.
- [6] Li, Y. J.; Wang, N.; Gan, H. Y.; Liu, H. B.; Li, H.; Li, Y. L.; He, X. R.; Huang, C. S.; Cui, S.; Wang, S.; Zhu, D. B. *J. Org. Chem.* **2005**, *70*, 9686.
- [7] Liu, Y.; Li, Y. J.; Jiang, L.; Gan, H. Y.; Liu, H. B.; Li, Y. L.; Zhuang, J. P.; Lu, F. S.; Zhu, D. B. *J. Org. Chem.* **2004**, *69*, 9049.
- [8] For selected examples, (a) Sinks, L. E.; Rybtchinski, B.; Iimura, M.; Jones, B. A.; Goshe, A. J.; Zuo, X. B.; Tiede, D. M.; Li, X. Y.; Wasielewski, M. R. *Chem. Mater.* **2005**, *17*, 6295; (b) Kelley, R. F.; Shin, W. S.; Rybtchinski, B.; Sinks, L. E.; Wasielewski, M. R. *J. Am. Chem. Soc.* **2007**, *129*, 3173.
- [9] For selected examples, (a) Kaiser, T. E.; Stepanenko, V.; Würthner, F. *J. Am. Chem. Soc.* **2009**, *131*, 6719; (b) Fischer, M. K. R.; Kaiser, T. E.; Würthner, F.; Bäuerle, P. *J. Mater. Chem.* **2009**, *19*, 1129.
- [10] Wang, H. Y.; Pu, K. Y.; Huang, S.; Liu, F.; Peng, B.; Wei, W. *React. Funct. Polym.* **2009**, *69*, 117.
- [11] Yoosaf, K.; James, P. V.; Ramesh, A. R.; Suresh, C. H.; Thomas, K. G. *J. Phys. Chem. C* **2007**, *111*, 14933.
- [12] Li, H.; Powell, D. R.; Hayashi, R. K.; West, R. *Macromolecules* **1998**, *31*, 52.
- [13] James, P. V.; Sudeep, P. K.; Suresh, C. H.; Thomas, K. G. *J. Phys. Chem. A* **2006**, *110*, 4329.
- [14] Sudeep, P. K.; James, P. V.; Thomas, K. G.; Kamat, P. V. *J. Phys. Chem. A* **2006**, *110*, 5642.
- [15] Ford, W. E.; Kamat, P. V. *J. Phys. Chem.* **1987**, *91*, 6373.
- [16] Würthner, F.; Thalacker, C.; Diele, S.; Tschiesske, C. *Chem. Eur. J.* **2001**, *7*, 2245.
- [17] Neuteboom, E. E.; Meskers, S. C. J.; van Hal, P. A.; van Duren, J. K. J.; Meijer, E. W.; Janssen, R. A. J.; Dupin, H.; Pourtois, G.; Cornil, J.; Lazzaroni, R.; Brédas, J. L.; Beljonne, D. *J. Am. Chem. Soc.* **2003**, *125*, 8625.
- [18] Würthner, F. *Chem. Commun.* **2004**, 1564.
- [19] Kimura, M.; NariKawa, H.; Ohta, K.; Hanabusa, K.; Shirai, H.; Kobayashi, N. *Chem. Mater.* **2002**, *14*, 2711.
- [20] Tominaga, M.; Suzuki, K.; Kawano, M.; Kusukawa, T.; Ozeki, T.; Sakamoto, S.; Yamaguchi, K.; Fujita, M. *Angew. Chem., Int. Ed.* **2004**, *43*, 5621.
- [21] Feyter, S. D.; Schryver, F. C. D. *J. Phys. Chem. B* **2005**, *109*, 4290.
- [22] Miura, A.; Chen, Z. J.; Uji-i, H.; De Feyter, S.; Zdanowska, M.; Jonkheijm, P.; Schenning, A. P. H. J.; Meijer, E. W.; Würthner, F.; De Schryver, F. C. *J. Am. Chem. Soc.* **2003**, *125*, 14968.

(Zhao, X.)